DOI: 10.32615/ps.2019.105 PHOTOSYNTHETICA 57 (4): 931-941, 2019

Selenium improves the transport dynamics and energy conservation of the photosynthetic apparatus of *in vitro* grown *Billbergia zebrina* (Bromeliaceae)

A.F.C. SOUZA, J.P.R. MARTINS+, A.B.P.L. GONTIJO, and A.R. FALQUETO

Department of Agrarian and Biological Sciences, Federal University of Espírito Santo, Litorâneo, 29932-540 São Mateus, ES, Brazil

Abstract

Despite having beneficial effects, selenium is not an essential element for plants and its action mechanisms are still unclear. In this context, we evaluated effects of selenium, considering possible modulations of the photosynthetic apparatus of *Billbergia zebrina* plants during *in vitro* culture. Lateral shoots of *B. zebrina* were grown in a medium with different concentrations of selenium (0, 2, 4, and 16 μM). After 75 d, concentrations of photosynthetic pigments, growth traits, and chlorophyll *a* fluorescence were evaluated. In low concentrations, selenium increased the potential energy conservation capacity of the photosynthetic apparatus, maintained the PSII energy transport reaction stability, and improved the electron transport dynamics between the intersystem and PSI. In addition, *B. zebrina* showed physiological disturbances at Se concentrations equal or greater than 16 μM, presenting reduced growth and photosynthetic pigment contents and impaired photosynthetic apparatus.

Additional key words: bromeliad; electron transport flux; fluorescence transient; JIP test; performance index; reaction center.

Introduction

Selenium (Se) is a nonessential element to plants. However, Se is known to have a beneficial effect when present in low concentrations (Pilon-Smith *et al*. 2009). Several studies have demonstrated multiple impacts of Se on plant physiology, such as increased biomass production (Chen *et al*. 2014, Jiang *et al*. 2015, Feng *et al*. 2016), delayed senescence (Xue *et al*. 2001), increased tolerance to oxidative damage (Feng *et al*. 2013, Diao *et al*. 2014, Qing *et al*. 2015, Tang *et al*. 2015), increased production of carotenoid pigments (Ning *et al*. 2016), higher tolerance to photooxidative stresses (Seppänen *et al*. 2003), greater carbohydrate accumulation (Turakainen *et al*. 2006, Owusu-Sekyere *et al*. 2013), and alleviation of the effects of biotic and abiotic stresses (Hanson *et al*. 2003, Yao *et al*. 2010, Hasanuzzaman and Fujita 2011, Han *et al*. 2015).

Plants vary substantially in their physiological responses to Se (Terry *et al*. 2000) and little is known about the possible mechanisms of action (Feng and Wei 2012). In this context, physiological increments caused by Se in plants can be attributed to several different mechanisms, such as reduced production of ROS, increased production of enzymatic and nonenzymatic antioxidants, recovery of damaged chloroplasts, and higher production of vital metabolites (Bachiega *et al*. 2016, Tian *et al.* 2016). The deficiency and toxicity of Se have been recorded worldwide, depending on its availability in the environment (Zhang *et al*. 2007). From the ecotoxicological standpoint, there is a narrow concentration range from which an element goes from beneficial to toxic (Pilon-Smits and LeDuc 2009, Zhu *et al.* 2009). Even low contamination, if present

Received 6 October 2018, *accepted* 25 June 2019.
+Corresponding author; phone: +55 27 3121 1696, e-mail: jprmartinss@yahoo.com.br
Abbreviations: ABS/RC – absorption flux per RC; Chl – chlorophyll; Chl_{total} – total chlorophyll; DI_0/RC – dissipated energy flux per RC; ET_0/RC – electron transport flux per RC; F_0 – minimal fluorescence yield of the dark-adapted state; F_I – fluorescence intensity at 30 ms; F_J – fluorescence intensity at 2 ms; F_K – fluorescence intensity at 0.3 ms; F_m – maximal fluorescence yield of the dark-adapted state; FM – fresh mass; F_P – fluorescence intensity at 300 ms; OCE – oxygen-evolving complex; Pheo – pheophytin; $PI_{(ABS)}$ – performance index based on absorption; $PI_{(Total)}$ – overall performance index, which measures the performance up until the final electron acceptors of PSI; RC – reaction center; RC/ABS – total number of active reaction center per absorption; RE_0/RC – reduction of end acceptors at PSI electron acceptor side per RC; ROS – reactive oxygen species; TR_0/RC – trapping flux per RC; V_I – relative variable fluorescence at 30 ms (point I); V_J – relative variable fluorescence at 2 ms (point J); δR_0 – efficiency/probability with which an electron from the intersystem electron carriers moves to reduce end electron acceptors at the PSI acceptor side; φD_0 – quantum yield of energy dissipation; φE_0 – quantum yield of electron transport; φP_0 – maximum quantum yield of primary photochemistry; φR_0 – quantum yield of reduction of end electron acceptors at the PSI acceptor side; ρR_0 – efficiency with which a trapped exciton can move an electron into the electron transport chain from Q_A^- to the PSI end electron acceptors; ψE_0 – probability that a trapped exciton moves an electron into the electron transport chain beyond Q_A^-.
Acknowledgments: The authors would like to acknowledge the scholarship awarded by the CNPq (Brazilian National Council for Scientific and Technological Development) and the FAPES (Espírito Santo State Research Foundation).

at a sufficiently large scale, can cause environmental damages (Lindblom *et al.* 2013). Hence, environmental contamination by Se can have an impact on human health, agricultural yield, and the stability of natural ecosystems.

High concentrations of Se can damage the photosynthetic apparatus, inhibit photosynthesis, and reduce starch production (Vítová *et al.* 2011, Łabanowska *et al.* 2012, Wang *et al.* 2012). However, in adequate concentrations, Se can enhance photosynthesis and protect the PSII (Feng *et al.* 2015, Jiang *et al.* 2015). Previous studies have shown that chlorophyll (Chl) *a* fluorescence analysis is an efficient nondestructive technique to evaluate modulations in the photosynthetic apparatus under different environmental conditions (Zushi *et al.* 2017). In the present study, the bromeliad, *Billbergia zebrina* (Herbert) Lindley, was chosen for *in vitro* cultivation. Analyses using *in vitro* cultures are advantageous since they allow isolating the effects of a particular substance on the plant metabolism in relation to all other potential stressing agents (Martins *et al.* 2016). Within this framework, the aim of this study was to evaluate the effect of Se on the photosynthetic performance of *in vitro* grown *B. zebrina* (Bromeliaceae), considering possible modulations (improvement, damage and/or changed site of action) in the photosynthetic apparatus, contributing to a better understanding of Se action in plants.

Materials and methods

Exposure of plant material to Se during *in vitro* growth: Lateral shoots of *B. zebrina*, obtained from plants previously established *in vitro*, were selected using a scalpel and transferred to 268-ml glass jars containing 50 ml of Murashige and Skoog plant growth medium (Murashige and Skoog 1962) supplemented with 30 g L^{-1} sucrose and solidified with 3.5 g L^{-1} agar. Selenium was added to the medium in exponential scale with the following concentrations: 0, 2, 4, and 16 µM. Sodium selenite (Na_2SeO_3) was used as a source of Se, considering the molecular mass of Se in all concentration calculations. The medium pH was adjusted to 5.8 before autoclaving at 120°C for 20 min. After inoculation under a laminar flow hood, the material was kept in a growth room for 75 d at 25 ± 2°C and a photoperiod of 16-h light/8-h dark.

Growth analysis: To evaluate the *in vitro* growth, 50 plants were randomly sampled from each treatment, divided into 10 parcels, and weighed on an analytical scale. The fresh mass (FM) of roots and aerial parts of the samples were determined separately.

Photosynthetic pigments content: To quantify the photosynthetic pigments, 0.03 g of plant material was extracted from the third completely expanded leaf in the central rosette region of 12 randomly selected samples. The plant material was placed in test tubes containing 5 ml of 80% acetone and kept in the dark at 4°C for 48 h, before spectrophotometric analysis. Readings were performed using a *GENESYS™ 10S* UV-Vis spectrophotometer (*Thermo Fisher Scientific*, West Palm Beach, FL, USA) at 645 and 665 nm for Chl *a* and Chl *b*, respectively. The contents of photosynthetic pigments, expressed in mg g^{-1}(FM), were calculated according to the equations of Arnon (1949) and Lichtenthaler (1987), as follows: Chl $a = [(12.7 \times A_{663}) \times (2.69 \times A_{645})/(1000 \times FM) \times V]$, Chl $b = [(22.9 \times A_{645}) \times (4.68 \times A_{663})/(1000 \times FM) \times V]$, and $Chl_{total} = [(20.2 \times A_{663}) \times (2.69 \times A_{645})/(1000 \times FM) \times V]$, where V = volume of the acetone extract in cm^3 and A = absorbance at the specified wavelength (nm), measured with a 1-cm cuvette.

Chl *a* fluorescence analysis: The Chl *a* fluorescence transient was measured after 75 d of cultivation. Measurements were performed in 15 plant samples per treatment, always in the third fully expanded leaf departing from the rosette's center. Leaves were previously adapted to the dark for 30 min using a leaf clips (*Hansatech*) to assure complete oxidation of the photosynthetic system. The transients were induced with 1 s of incident light for a saturating light pulse with maximum intensity of 3,000 µmol(photon) m^{-2} s^{-1} in a leaf area of 4 mm in diameter using a portable fluorometer (*Handy PEA*, *Hansatech Instruments Ltd*., King's Lynn, Norfolk, UK). Emission of the transient fluorescence was then registered from 10 ms to 1 s with 120 fluorescence points. From the fluorescence transient curve OJIP, the JIP test was evaluated according to the theory of energy flow across biomembranes (Strasser and Strasser 1995, Strasser *et al.* 2004) considering the parameters cited in Appendix.

Statistical analysis: Experiments were performed in a completely randomized design. The parameters of the JIP test, photosynthetic pigments, and fresh mass (FM), were submitted to analysis of variance (*ANOVA*) and the means were compared using *Scott-Knott*'s test at 5% significance. Analyses were performed using the software *SISVAR*.

Results

Significant reductions were observed in the FM of both roots and aerial parts of the plants treated with 16 µM Se,

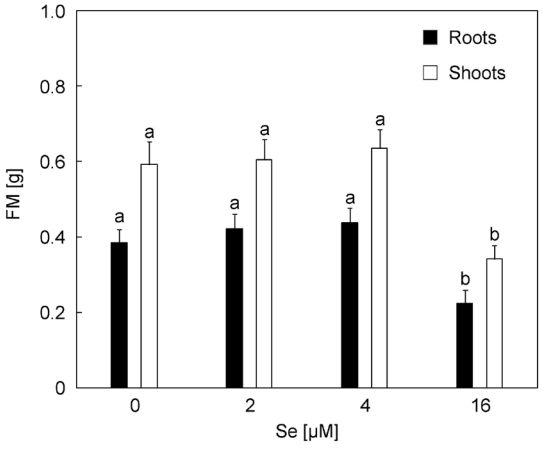

Fig. 1. Growth traits of *in vitro* grown *Billbergia zebrina* plants as a function of Se concentrations (0, 2, 4, and 16 µM). For each growth trait, means ± SD (n = 10) followed by *the same letter* are not significantly different according to the *Scott-Knott*'s test (p<0.05). FM – fresh mass.

without significant effects of the other treatments (Fig. 1). Similarly, the concentration of Chl *a* and Chl_{total} decreased under 16 μM Se without any alteration in the concentration of Chl *b* among the Se concentrations (Table 1). Samples of *B. zebrina*, when submitted to treatments of Se *in vitro*, remained photosynthetically active and the curves had a typical OJIP polyphasic increase (Fig. 2*A*). Relative to the control, there was a decrease in F_0 and of the obtained fluorescence at 0.3 ms (F_K) in the samples cultivated with 2 and 4 μM Se. On the other hand, higher values of F_0 and F_K were obtained in plants grown with 16 μM (Fig. 2*A*). Suppressions of the fluorescence signs obtained at 2 ms and 300 ms (F_J and F_P, respectively) occurred in all Se treatments, including point I (obtained at 30 ms). However,

Table 1. Content of chlorophyll *a* (Chl *a*), chlorophyll *b* (Chl *b*), and total chlorophyll (Chl_{total}) of *in vitro* grown *Billbergia zebrina* plants as a function of Se concentrations (0, 2, 4, and 16 μM). For each pigment, means ± SD (n = 12) followed by *the same letter* in the column are not significantly different according to *Scott-Knott*'s (p<0.05). FM – fresh mass.

Se [μM]	Chl *a* [mg g^{-1}(FM)]	Chl *b* [mg g^{-1}(FM)]	Chl_{total} [mg g^{-1}(FM)]
0	1.11 ± 0.06[a]	0.42 ± 0.04[a]	1.83 ± 0.10[a]
2	1.06 ± 0.06[a]	0.48 ± 0.02[a]	1.75 ± 0.09[a]
4	1.09 ± 0.03[a]	0.44 ± 0.01[a]	1.79 ± 0.05[a]
16	0.91 ± 0.05[b]	0.38 ± 0.04[a]	1.49 ± 0.08[b]

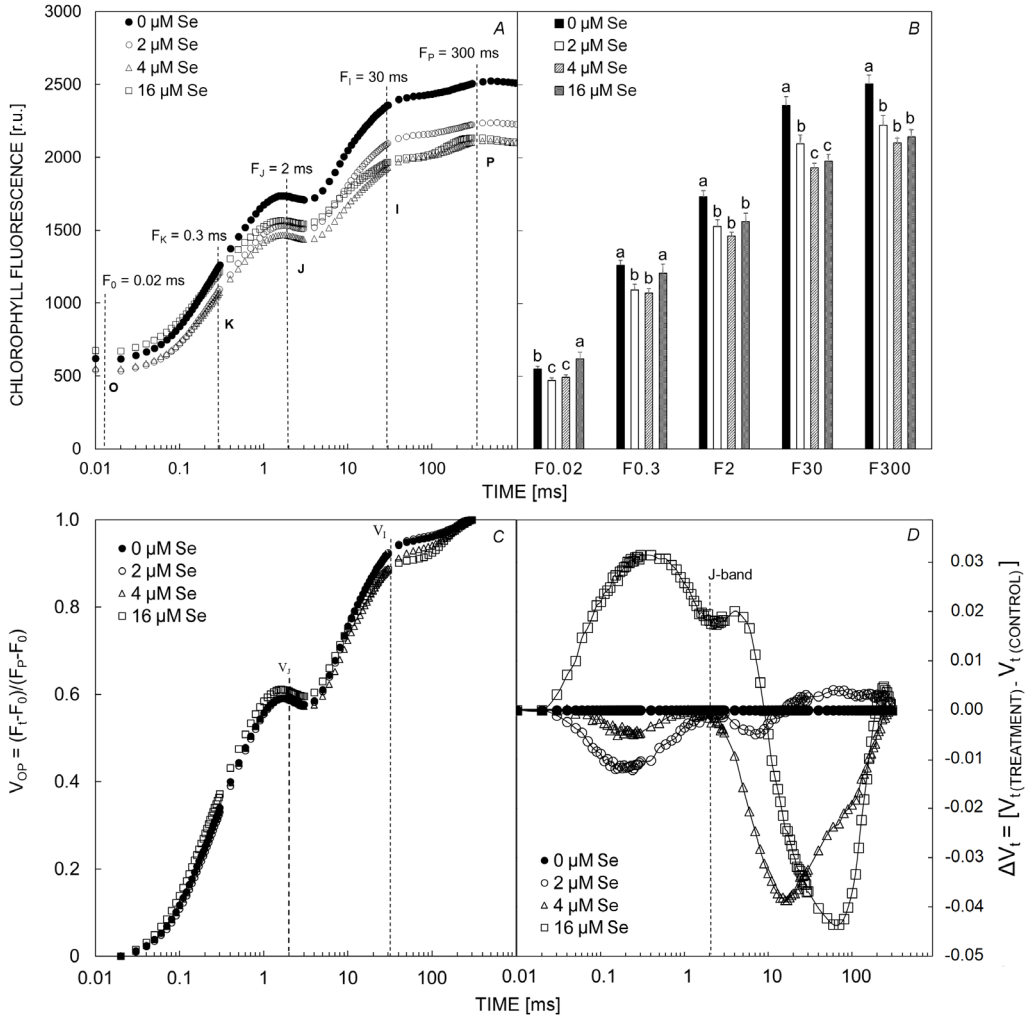

Fig. 2. Effects of different concentrations of selenium (0, 2, 4, and 16 μM) on the polyphase emission curve of chlorophyll *a* fluorescence (*A*); OJIP transient points (O = 0.02 ms, K = 0.3 ms, J = 2 ms, I = 30 ms, and P = 300 ms) (*B*); relative fluorescence between points 0.02 and 300 ms or $V_{OP} = (F_t - F_0)/(F_m - F_0)$ (*C*); and kinetic differences between O (0.02 ms) and P (300 ms) or ΔV_{OP} values established between 0.01 and 300 ms (*D*) in *Billbergia zebrina* plants grown *in vitro*. For each OJIP transient point, means ± SD (n = 15) followed by *the same letter* are not significantly different according to the *Scott-Knott*'s test (p<0.05).

a higher suppression of point I was observed in the samples treated with 4 µM and 16 µM Se (Fig. 2*B*).

Increases in V_J were observed in the samples treated with 16 µM Se followed by suppression of V_I in plants cultured with 4 and 16 µM Se (Fig. 2*C*). Using the relative normalizations at ΔV_t, established between 0.02 and 300 ms, a positive deviation was observed in the samples cultivated with 16 µM Se at 2 ms, while for those treated with 2 and 4 µM Se, no deviation was observed (Fig. 2*D*). However, in the phases included between points J and P, negative differences were obtained at 30 ms (I-band) to the treatments with 4 and 16 µM Se (Fig. 2*D*).

Negative differences were observed in the L-band and K-band (ΔV_{OK} and ΔV_{OJ} established between 0–0.3 and 0–2 ms, respectively) in the samples cultivated with 2 and 4 µM Se, being more pronounced (higher negative amplitude) in those with lower concentrations (Fig. 3*A*). On the other hand, plants cultivated with 16 µM Se showed positive differences in the L-band and K-band (+0.026 and +0.061, respectively) compared to the control (Fig. 3).

The curves of higher amplitude observed to the relative fluorescence at $V_{OI} \geq 1.0$, obtained in the interval of 30 and 300 ms, were observed for 4 and 16 µM Se (Fig. 4*A*), as well as taking longer to reach 0.5 in the V_{IP} coordinate established in the same time lapse, but considering F_J and F_P (Fig. 4*B*). The $\Delta V_{IP} = (F_p - F_I)/(F_p - F_0)$ increased gradually in plants cultivated with 4 and 16 µM Se (Fig. 4*B*). The curves regarding the relative fluorescence variable between points I–P or $\Delta V_{IP} = (V_{IP(treatment)} - V_{IP(control)})$ were negative in relation to the control in the treatments with 4 and 16 µM Se (Fig. 4*C*).

The specific energy fluxes extracted from the JIP test evidenced reductions in RC/ABS of plants grown with 16 µM Se. Hence, the values of ABS/RC were higher and differed significantly from the other treatments. Similarly, with 16 µM Se, higher values of TR_0/RC and DI_0/RC were observed. No difference in ET_0/RC was registered between the treatments, while RE_0/RC increased significantly in the plants cultivated with 4 and 16 µM Se (Fig. 5).

The $\varphi P_0 = TR_0/ABS$ was higher and equivalent at 0, 2, and 4 µM Se, differing from the treatments using 16 µM Se. Therefore, with 16 µM Se, higher values of $\varphi D_0 = DI_0/ABS$ were observed, since these are inversely proportional parameters (Fig. 6*A*). On the other hand, lower values of $\varphi E_0 = ET_0/ABS$ were observed in plants cultivated with 16 µM. For $\psi E_0 = ET_0/TR_0$, no differences were observed between the Se concentrations. Higher values of $\varphi R_0 = RE_0/ABS$, $\delta R_0 = RE_0/ET_0$, and $\rho R_0 = RE_0/TR_0$ were observed for the treatments with 4 and 16 µM Se (Fig. 6*A*). Higher values of $PI_{(ABS)}$ were observed at 0, 2, and 4 µM Se (Fig. 6*B*), differing from those obtained with 16 µM Se. For $PI_{(Total)}$, the highest index observed was for 4 µM Se (Fig. 6*C*).

Discussion

The plants grown in the treatments with 0, 2, and 4 µM Se did not show any difference in FM (Fig. 1). For alfalfa (Broyer *et al.* 1966), ryegrass (Hartikainen *et al.* 1997), and sorghum (Djanaguiraman *et al.* 2010), low concentrations of Se have also shown positive effects on plant growth. The capacity of Se to promote growth has been reported also in lettuce (Xue *et al.* 2001) and soybean (Djanaguiraman *et al.* 2005). In general, these studies have shown that the high concentrations of Se reduce growth, as observed in *B. zebrina* plants cultivated with 16 µM Se (Fig. 1). According to Hartikainen *et al.* (2000) and Djanaguiraman *et al.* (2005), the effects of Se on plant growth can be attributed especially to the antioxidative function of Se, mediated by selenoproteins such as glutathione peroxidase. These compounds catalyze the reduction of hydroperoxidases with glutathione, protecting against oxidative damages (Stadtman *et al.* 1996, Kryukov *et al.* 2003).

The quantification of the photosynthetic pigments in plant tissues under different environmental conditions can be an important tool for ecophysiological evaluation

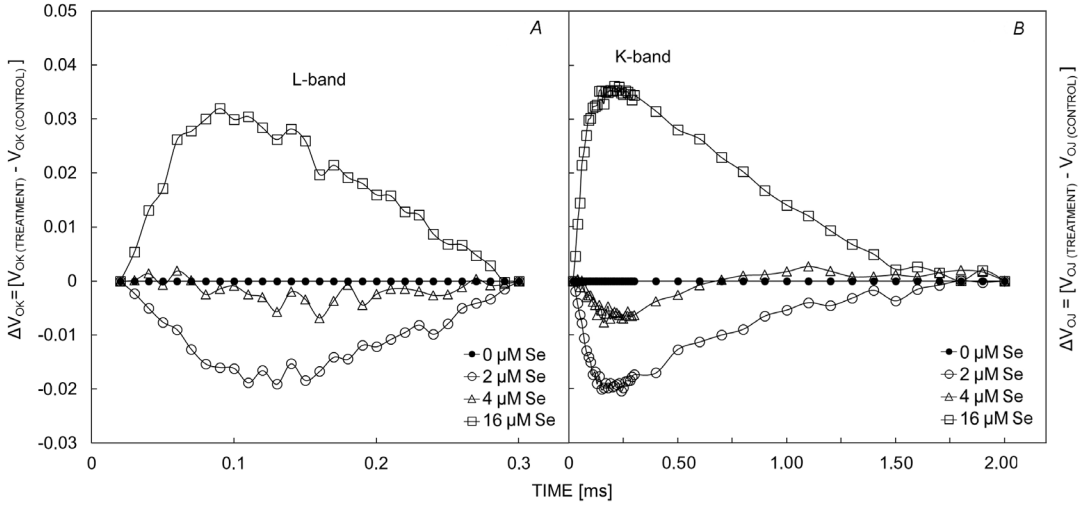

Fig. 3. Chlorophyll *a* fluorescence transient points (n = 15) between the O–J and J–I stages of *Billbergia zebrina* plants grown in a medium with different Se concentrations. The kinetic differences between steps O and K showing the L-band (*A*) and the kinetic differences between steps O and J showing the K-band (*B*).

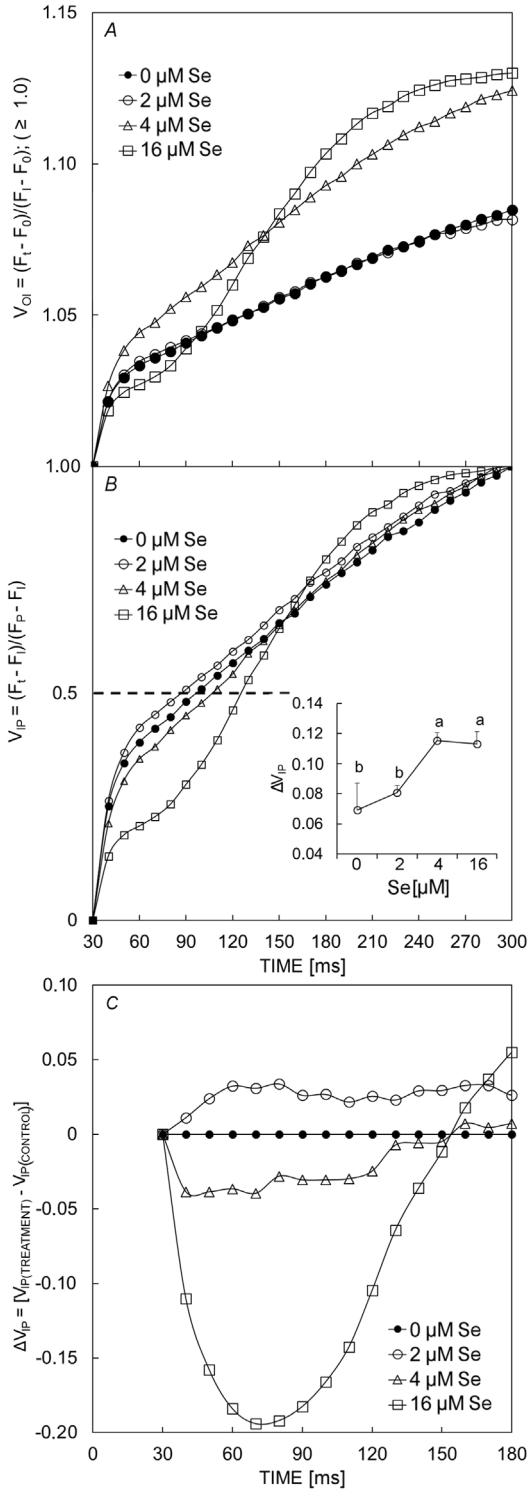

Fig. 4. Normalization between F_0 and F_I where $V_{OI} = (F_t - F_0)/(F_I - F_0)$, where $V_{OI} \geq 1$ is in the range of 30 to 300 ms (*A*); normalization between F_I and F_P where $V_{IP} = (F_m - F_I)/(F_m - F_0)$ (*B*); and relative variable fluorescence between the I–P points or ΔV_{IP} (*C*) in *Billbergia zebrina* plants grown *in vitro* with different concentrations of selenium (0, 2, 4, and 16 µM). Means ± SD (n = 15) followed by *the same letter*, shown in the V_{IP} chart, are not significantly different according to the *Scott-Knott*'s test (p<0.05).

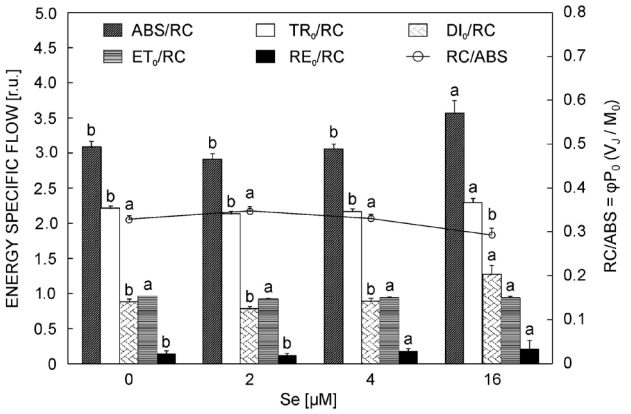

Fig. 5. Photochemical parameters derived from the analysis of the JIP test [ABS/RC – absorption flux per reaction center (RC); DI_0/RC – dissipated energy flux per RC; ET_0/RC – electron transport flux per RC; RC/ABS – total number of active reaction center per absorption; RE_0/RC – reduction of end acceptors at PSI electron acceptor side per RC; TR_0/RC – trapping flux per RC] of *in vitro* grown *Billbergia zebrina* plants as a function of Se concentration (0, 2, 4, and 16 µM). For each JIP test parameter, means ± SD (n = 15) followed by *the same letter* are not significantly different according to the *Scott-Knott*'s test (p<0.05).

(Lambers *et al.* 2008). The photosynthetic pigments control the quantity of solar radiation that is absorbed by plants and other photosynthetic organisms. This makes the pigments intimately associated with the photosynthetic rates and the primary yield during the photosynthetic photochemical phase (Blackburn 2007).

Plants of *B. zebrina* cultivated with 2 and 4 µM Se, although not varying in the contents of photosynthetic pigments (Table 1), showed modulations in the photosynthetic apparatus when compared to the control. Plants cultured with 16 µM Se presented a decrease in the Chl_{total} content (Table 1). Therefore, these plants could undergo a photodestructive effect caused by the greater degradation rates and reduction in the biosynthesis of these pigments (Tausz *et al.* 2001), possibly related to the toxic effect of the high concentrations of Se (Zhong *et al.* 2015).

The increase in the magnitude of the fluorescence signals from the basal (F_0) to the maximum level (F_m), with well-established intermediate points J and I, indicated that the samples were photosynthetically active in all treatments (Mehta *et al.* 2010, Yusuf *et al.* 2010) (Fig. 2*A*). The suppression of all reference points of the OJIP transient (0.02, 0.3, 2, 30, and 300 ms) with 2 and 4 µM Se (Fig. 2*B*) likely indicate greater allocation of energy to photochemical quenching, given that there was no difference in terms of heat dissipation (DI_0/RC) for these treatments (Fig. 5).

In the present study, the increase in V_J observed in the plants cultivated with 16 µM Se (Fig. 2*C*) suggests an accumulation of reduced quinone A (Q_A^-), which leads to deceleration in the electron transfer to the second acceptor of the electron transport chain, quinone B (Q_B) (Strasser *et al.* 2000, Chen *et al.* 2014). The kinetic difference (ΔV_t), which appears around 2 ms (Fig. 2*D*), is strongly

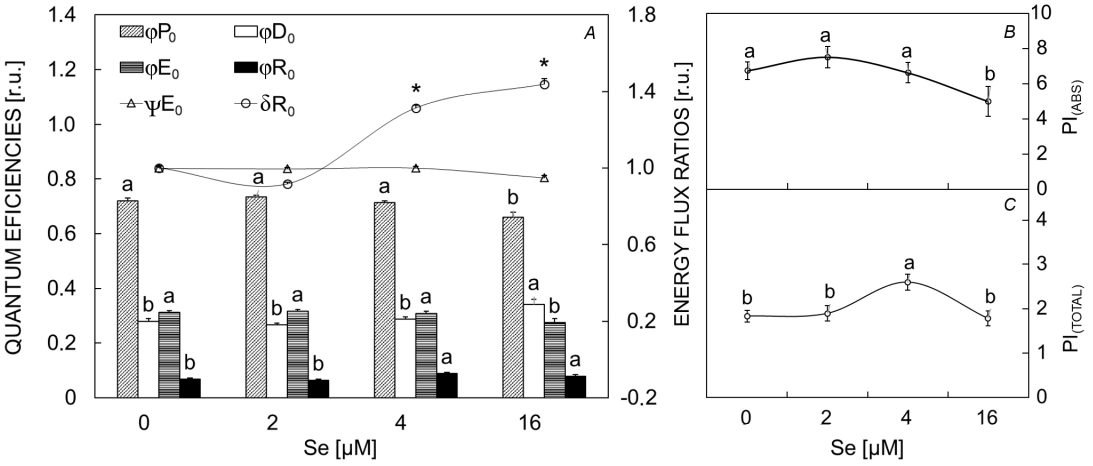

Fig. 6. Photochemical parameters derived from the analysis of the JIP test (ψE_0 – probability that a trapped exciton moves an electron into the electron transport chain beyond Q_A^-; φD_0 – quantum yield of energy dissipation; φE_0 – quantum yield of electron transport; φP_0 – maximum quantum yield of primary photochemistry; φR_0 – quantum yield of reduction of end electron acceptors at the PSI acceptor side; δR_0 – efficiency/probability with which an electron from the intersystem electron carriers moves to reduce end electron acceptors at the PSI acceptor side) of *in vitro* grown *Billbergia zebrina* plants as a function of Se concentration (0, 2, 4, and 16 μM) (*A*). *The lines* (secondary ordinate scale on the right) represent the normalized values according to the control (0 μM). The asterisk (*) represents a difference between the treatments with selenium in relation to the control according to the *Scott-Knott*'s test (p<0.05). Performance index based on absorption ($PI_{(ABS)}$) (*B*) and overall performance index, which measures the performance up until the final electron acceptors of PSI ($PI_{(Total)}$) (*C*) of *Billbergia zebrina* plants under Se treatments. In all graphs, means ± SD (n = 15) followed by *the same letter* are not significantly different according to the *Scott-Knott*'s test (p<0.05).

influenced by the redox reactions of the initial acceptors, especially Q_A (Strasser *et al.* 2010, Krüger *et al.* 2014). Hence, a positive band, such as that observed in the samples cultivated in the presence of 16 μM Se, suggests that high concentrations of Se reduce the probability of electrons moving from the intersystem to the PSI from the Q_A^- (Strasser *et al.* 2000). On the other hand, for the *B. zebrina* plants cultivated in all other Se treatments, there was no difference in relation to the control (Fig. 2*D*). This result likely indicates stability in the water electron donation in relation to an increase or maintenance of the PSI activity, as observed by Krüger *et al.* (2014) in studies with different temperatures. Or, as suggested by Christen *et al.* (2007) in studies with grapevines under biotic and abiotic stress, a negative J-band may suggest an increase in the capacity to reoxidize the pool of quinones.

According to Oukarroum *et al.* (2009), analyses of both L- and K-bands are good references to characterize physiological disturbances in plants. The L-band, which appears at approximately 0.15 ms, indicates energetic connectivity (grouping) of the PSII units (Strasser *et al.* 2004). Therefore, a positive L-band, such as that observed in plants cultivated with 16 μM Se (Fig. 3*A*), suggests that high concentrations of Se make the energetic cooperation among the PSII units less stable (Pollastrini *et al.* 2017). Such phenomenon is likely associated with disorganization in the thylakoid membranes (Oukarroum *et al.* 2007). However, the negative differences observed in the plants submitted to 2 and 4 μM Se indicate stronger connectivity (Fig. 3*A*), which results in better use of the excitement energy and higher stability of the system (Strasser *et al.* 2004).

The K-band appears at approximately 0.3 ms (Fig. 3*B*) and expresses the electron donation activity from the oxygen-evolving complex (OEC) to the PSII, which accordingly competes with electron donations not coming from water (Pollastrini *et al.* 2017). A positive K-band, such as the one observed in plants grown with 16 μM Se (Fig. 3*B*), indicates loss of OEC integrity, weakening the stability of oxygen evolution by the Mn_4CaO_5 complex as an electron donor to the PSII (Gururani *et al.* 2012).

Strasser *et al*. (2000) reported alteration in the OEC, enabling alternative electron donors to transfer electrons to the PSII, leading to an increase in the $Pheo^-$ and Q_A^-, and therefore generating a positive K-band. Since the OEC gives access to electron donors not coming from water, such as ascorbate (Tóth *et al.* 2011), proline (De Ronde *et al.* 2004) or any other internal donor with an electropotential more negative than the H_2O/O_2 reaction, its malfunctioning can be compensated by these donors for a short period of time (Gururani *et al.* 2012). Positive values for the K-band may also indicate an increase in the functional antenna size associated with the PSII (Yusuf *et al.* 2010), as well as damages between the donor and acceptor sides of the PSII, resulting from an imbalance between the OEC electron flow to the reaction center and the acceptor side of the PSII towards the PSI (Strasser 1997, Chen and Cheng 2010). A negative K-band, such as those observed in plants grown with 2 and 4 μM Se in relation to the control (Fig. 3*B*), indicates an increase in the OEC functioning and integrity of the Mn_4CaO_5 complex. This condition could restrict the entrance of electrons not coming from water, thus causing higher efficiency of the OEC in the donation of electrons to the PSII (De Ronde *et al.* 2004). The I–P phase refers to the events of electron transfer associated with the PSI (Schansker *et al.* 2003, Redillas *et al.* 2011), and it was

the stage of highest influence of Se on photosynthetic apparatus in the analyzed samples. The curves $V_{OI} \geq 1.0$ of higher amplitude observed in the treatments with 4 and 16 μM Se (Fig. 4*A*) are also an indication of the dynamic modulations of the electron transport from the intersystem to the PSI (Yusuf *et al.* 2010). In addition, it also suggests an increase in the pool size of the final electron acceptors from the acceptor side of the PSI. The largest values of ΔV_{IP} were also observed in these treatments (Fig. 4*B*), indicating a higher contribution relative to the I–P phase to the curve of emission of the Chl *a* fluorescence and the abundance of units of the PSI (Ceppi *et al.* 2012). Schansker *et al*. (2005) demonstrated that the increase in the relative contribution of the I–P phase to the fluorescence curve depends both on the electron flow through the PSI and blockage of the electron flow in the acceptor side of the PSI.

The normalization V_{IP} allows a deduction in the electron flow behavior coming from the intersystem to the final acceptors of the PSI (Martins *et al.* 2017), thus enabling an estimation of the global rate of reduction of the final acceptors of the PSI (Fig. 4*B*). Plants cultivated with 4 and 16 μM Se presented a decrease in V_{IP} (Fig. 4*B*), as described by the Michaelis-Menten equation, where the inverse of the time to reach $V_{IP} = 0.5$ is the determinant of the decrease in the reducing capacity of the PSI (Yusuf *et al.* 2010). The data from the plants cultivated with 4 and 16 μM Se suggest that addition of Se to the growth medium does not imply proportionality between the global rate of reduction of the final receptors of the PSI and the amount of time and light necessary to reach 50% of the emission of the I–P phase (determined by the relative variable fluorescence between points I–P or ΔV_{IP}) (Yusuf *et al.* 2010, Martins *et al.* 2017) (Fig. 4*B*,*C*). However, this demand for time and light encountered by the analysis of ΔV_{IP} seems proportional to an increase in PSI units and relative contribution of the I–P phase to the Chl *a* fluorescence emission curve, as observed in the samples cultivated with 4 and 16 μM Se (Fig. 4*B*,*C*). Accordingly, Se can induce an increase in the PSI activity. The importance of these mechanisms is in the photooxidative reduction, directing electrons to alternative routes to the electron cyclic flow involving the PSI, thus decreasing the formation of ROS (Oukarroum *et al.* 2015) and increasing the ferredoxin-Fd reductase, other intermediates, and $NADP^+$ (Yusuf *et al.* 2010, Redillas *et al.* 2011).

The parameters of the JIP test derived from the OJIP transients can be used to characterize the behavior/activity of the PSII, intersystem, and PSI (Strasser *et al.* 2004, Strauss *et al.* 2006, Tsimilli-Michael and Strasser 2013). These parameters are considered efficient in targeting different sites of action and the heterogeneity of the PSII (Appenroth *et al.* 2001, Kalaji *et al.* 2014). For example, the increase in ABS/RC with 16 μM Se can be attributed to two factors. The first is the increase in the functional antenna size associated with the PSII, which provides the reaction centers with excitement energy (Yusuf *et al.* 2010). Since the TR_0/RC increased proportionally to ABS/RC in plants cultivated with 16 μM Se, it is possible to suggest a weakening in the dynamics of electron transport from OEC to the PSII (Chen *et al.* 2014, Kalaji *et al.* 2014), as well as the transfer of excitement energy from the inactive to the active reaction centers (Lavergne and Leci 1993) (Fig. 5). In plants cultivated with 16 μM Se, there was also a decrease in RC/ABS (Fig. 5), a parameter that indicates the stability of the reaction centers and their connection to other light-harvesting antenna complexes (Chen *et al.* 2014). This condition implies the second factor for the increase in ABS/RC, *i.e*., the inactivation of a fraction of the active reaction centers, transforming them into nonreducers of Q_A (Yusuf *et al.* 2010, Redillas *et al.* 2011).

Decreases in RC/ABS can be an indication of susceptibility to photoinhibition and formation of silent reaction centers (Chen *et al.* 2014). Accordingly, it can be inferred that the size of the ABS/RC and TR_0/RC associated with the increase in DI_0/RC observed after the growth of plants with 16 μM Se characterizes a structural transformation in the reaction centers into units that dissipate excitement energy in the form of heat (Strasser *et al.* 2004) (Fig. 5). This condition could avoid the overproduction of Q_A^- (Redillas *et al.* 2011) and reduce the formation of ROS, thus protecting the excitement system and excessive reduction (Chen *et al.* 2014). The sequence of parameters that characterize the transduction of energy from the reaction centers or the PSII is the absorption (ABS/RC), capture (TR_0/RC), and transport of electrons (ET_0/RC). In the present study, no alterations were observed to the JIP test parameters in treatments with low Se concentrations (2 and 4 μM) (Fig. 5). Finally, the analysis of RE_0/RC values, related to the reduction of the final acceptors of the PSI, allowed verifying the significant increases obtained with 4 and 16 μM Se (Fig. 5). These results indicate an increase in the contribution in the I–P phase to the OJIP transient, corroborating the observations of Oukarroum *et al.* (2009) and Paillotin (1976). Within these Se concentrations, the electron transport capacity between Q_A^- and the PSI acceptors was increased.

In this study, decreases in the photochemical quantum yield of the PSII were obtained from the plants cultivated with 16 μM Se, which according to Hermans *et al.* (2003) can be related to the conversion of the Q_A reducing center into nonreducing or dissipating centers (Fig. 6*A*), as described previously when analyzing the results obtained for ABS/RC, RC/ABS, and DI_0/RC (Fig. 5). Decreases in φP_0 can be considered indicative of photoinhibitory damages to the PSII complex (Baker and Rosenqvist 2004). This condition can alter the shape of the OJIP curves, either by decreasing F_m or by increasing F_0 (Lin *et al.* 2009), as observed in plants grown with 16 μM Se (Fig. 6*A*). According to Oukarroum *et al.* (2009), these alterations reduce the efficiency by which an absorbed photon can be captured by the reaction center of the PSII. All these structural parameters of the JIP test characterize the events related to the PSII structure and intersystem (φP_0, φD_0, and φE_0) or O–J and J–I phases, respectively (Strasser *et al.* 2004, Tsimilli-Michael and Strasser 2008), which did not differ between the Se concentrations of 0, 2, and 4 μM (Fig. 6*A*). Hence, this result suggests that at these concentrations of Se, the stability of the PSII and intersystem is maintained without any signs of increase or

decrease. On the contrary, the lower values observed for φP_0 and φE_0 followed by an increase in φD_0 in the plants cultivated with 16 μM Se reinforces the occurrence of photoinhibition (Fig. 6*A*), indicating a reduction in the dynamics of transport and use of excitement energy (Zhuo *et al.* 2017), and therefore limiting the growth of *B. zebrina* at higher Se concentrations. Increases in the electron transfer across the intersystem to the reduction of the final acceptors of PSI occurred in the *B. zebrina* plants grown with 4 and 16 μM Se in relation to all other treatments (Fig. 6*A*). The intersystem and PSI can be potential sites of action for Se. This inference is based on the increase in the efficiency in the electron transfer from the reduced plastoquinone to the PSI acceptor side, evaluated by means of the δR_0 parameter analysis (Oukarroum *et al.* 2009), observed in the plants grown with 4 and 16 μM Se (Fig. 6*A*). Also, increases in these treatments were also observed when the quantum yield was evaluated regarding reduction of the final acceptors of the PSI (Tsimilli-Michael and Strasser 2008) (Fig. 6*A*). This increase in stability with reduction of PSI final acceptors attributed to Se most likely indicates an increase in the number of reaction centers associated with the PSI (Oukarroum *et al.* 2009).

Finally, the indexes of vitality ($PI_{(ABS)}$ and $PI_{(Total)}$) represent a product of some independent functional and structural parameters (Strasser *et al.* 2004, Kalaji *et al.* 2016). Higher values of PI indicate an increase in the potential energy conservation ability of the photosynthetic apparatus (Yusuf *et al.* 2010). Similarity of the $PI_{(ABS)}$ values of plants cultivated with 0, 2, and 4 μM Se indicate that selenium maintains the potential capacity of energy conservation for the reduction of the electron acceptors to the intersystem (Yusuf *et al.* 2010, Redillas *et al.* 2011, Krüger *et al.* 2014, Chen *et al.* 2015) (Fig. 6*B*). With respect to the $PI_{(Total)}$, only the plants grown with 4 μM Se had increases in the energy conservation capacity of the photosynthetic apparatus (Fig. 6*C*). $PI_{(Total)}$ encompasses, in addition to $PI_{(ABS)}$, the likelihood that an electron from the intersystem moves to reduce the final acceptors on the acceptor side of the PSI (δR_0) (Tsimilli-Michael and Strasser 2008), in which increases were observed (approximately 30%) of plants cultivated with 4 μM Se. This increase in δR_0 made the $PI_{(Total)}$ values of plants grown with 4 μM Se more pronounced and suggests, again, that the site of action of selenium may be between the intersystem and the PSI (Fig. 6*C*). Since $PI_{(Total)}$ incorporated parameters that characterize all the phases of the OJIP, it is considered by several authors to be the most sensitive JIP test parameter to characterize the physiological state of plants under different abiotic conditions (Strasser *et al.* 2004, Oukarroum *et al.* 2007, Yusuf *et al.* 2010, Brestič and Živčák 2013, Kalaji *et al.* 2014).

Conclusion: This study demonstrated that at 2 and 4 μM Se, the stability of the energy transport reaction in the PSII in *B. zebrina* were maintained. Furthermore, the potential capacity of energy conservation in the photosynthetic apparatus ($PI_{(Total)}$) was improved at 4 μM Se. The enhancement of the electron transport dynamics from the intersystem to the PSI (evaluating δR_0 and φR_0) reported to the higher Se concentrations suggests the PSI the mainly site of action of Se within the photosynthetic apparatus. Accordingly, using *B. zebrina* as a model, we can infer that at 2 and 4 μM Se can cause increases in the structure and functionality of the photosynthetic apparatus. In addition, we observed that *B. zebrina* showed physiological disturbances at 16 μM Se, displaying impaired growth and photosynthetic pigments content, and instability in the structure and functionality of the photosynthetic apparatus, especially in the PSII. Hence, from the ecotoxicological standpoint, the excess of Se was toxic to the studied species.

References

Appenroth K.J., Stöckel J., Srivastava A., Strasser R.J.: Multiple effects of chromate on the photosynthetic apparatus of *Spirodela polyrhiza* as probed by OJIP chlorophyll *a* fluorescence measurements. – Environ. Pollut. **115**: 49-64, 2001.

Arnon D.I.: Copper enzymes in isolated chloroplasts. Polyphenoloxidase in *Beta vulgaris*. – Plant Physiol. **24**: 1-15, 1949.

Bachiega P., Salgado J.M., de Carvalho J.E. *et al.*: Antioxidant and antiproliferative activities in different maturation stages of broccoli (*Brassica oleracea* Italica) biofortified with selenium. – Food Chem. **190**: 771-776, 2016.

Baker N.R., Rosenqvist E.: Applications of chlorophyll fluorescence can improve crop production strategies: an examination of future possibilities. – J. Exp. Bot. **55**: 1607-1621, 2004.

Blackburn G.A.: Hyperspectral remote sensing of plant pigments. – J. Exp. Bot. **58**: 855-867, 2007.

Brestič M., Živčák M.: PSII fluorescence techniques for measurement of drought and high temperature stress signal in crop plants: protocols and applications. – In: Das A.B., Rout G.R. (ed.): Molecular Stress Physiology of Plants. Pp. 87-131. Springer, New Delhi 2013.

Broyer T.C., Lee D.C., Asher C.J.: Selenium nutrition of green plants. Effect of selenite supply on growth and selenium content of alfalfa and subterranean clover. – Plant Physiol. **41**: 1425-1428, 1966.

Ceppi M.G., Oukarroum A., Çiçek N. *et al.*: The IP amplitude of the fluorescence rise OJIP is sensitive to changes in the photosystem I content of leaves: a study on plants exposed to magnesium and sulfate deficiencies, drought stress and salt stress. – Physiol. Plantarum **144**: 277-288, 2012.

Chen L.S., Cheng L.: The acceptor side of photosystem II is damaged more severely than the donor side of photosystem II in 'Honeycrisp' apple leaves with zonal cholorosis. – Acta Physiol. Plant. **32**: 253-261, 2010.

Chen Q., Guan T., Yun L. *et al.*: Online forecasting chlorophyll *a* concentrations by an auto-regressive integrated moving average model: Feasibilities and potentials. – Harmful Algae **43**: 58-65, 2015.

Chen S.G., Strasser R.J., Qiang S.: *In vivo* assessment of effect of phytotoxin tenuazonic acid on PSII reaction centers. – Plant Physiol. Bioch. **84**: 10-21, 2014.

Christen D., Schönmann S., Jermini M. *et al.*: Characterization and early detection of grapevine (*Vitis vinifera*) stress responses to esca disease by *in situ* chlorophyll fluorescence and comparison with drought stress. – Environ. Exp. Bot. **60**: 504-514, 2007.

De Ronde J.A., Cress W.A., Krüger G.H.J. *et al.*: Photosynthetic response of transgenic soybean plants, containing an *Arabidopsis P5CR* gene, during heat and drought stress. – J. Plant Physiol. **161**: 1211-1224, 2004.

Diao M., Ma L., Wang J. *et al.*: Selenium promotes the growth

and photosynthesis of tomato seedlings under salt stress by enhancing chloroplast antioxidant defense system. – J. Plant Growth Regul. **33**: 671-682, 2014.

Djanaguiraman M., Durga Devi D., Shanker A.K. *et al*.: Selenium: an antioxidative protectant in soybean during senescence. – Plant Soil **272**: 77-86, 2005.

Djanaguiraman M., Prasad P.V.V., Seppänen M.: Selenium protects sorghum leaves from oxidative damage under high temperature stress by enhancing antioxidant defense system. – Plant Physiol. Bioch. **48**: 999-1007, 2010.

Feng R.W., Liao G.J., Guo J.K. *et al*.: Responses of root growth and antioxidative systems of paddy rice exposed to antimony and selenium. – Environ. Exp. Bot. **122**: 29-38, 2016.

Feng R.W., Wei C.Y.: Antioxidative mechanisms on selenium accumulation in *Pteris vittata* L., a potential selenium phytoremediation plant. – Plant Soil Environ. **58**: 105-110, 2012.

Feng R.W., Wei C.Y., Tu S.X.: The roles of selenium in protecting plants against abiotic stresses. – Environ. Exp. Bot. **87**: 58-68, 2013.

Feng T., Chen S.S., Gao D.Q. *et al*.: Selenium improves photosynthesis and protects photosystem II in pear (*Pyrus bretschneideri*), grape (*Vitis vinifera*), and peach (*Prunus persica*). – Photosynthetica **53**: 609-612, 2015.

Gururani M.A., Upadhyaya C.P., Strasser R.J. *et al*.: Physiological and biochemical responses of transgenic potato plants with altered expression of PSII manganese stabilizing protein. – Plant Physiol. Bioch. **58**: 182-194, 2012.

Han D., Xiong S.L., Tu S.X. *et al*.: Interactive effects of selenium and arsenic on growth, antioxidant system, arsenic and selenium species of *Nicotiana tabacum* L. – Environ. Exp. Bot. **117**: 12-19, 2015.

Hanson B., Garifullina G.F., Lindblom S.D. *et al*.: Selenium accumulation protects *Brassica juncea* from invertebrate herbivory and fungal infection. – New Phytol. **159**: 461-469, 2003.

Hartikainen H., Ekholm P., Piironen V. *et al.*: Quality of the ryegrass and lettuce yields as affected by selenium fertilization. – Agr. Food Sci. Finland **6**: 381-387, 1997.

Hartikainen H., Xue T.L., Piironen V.: Selenium as Na antioxidant and pro-oxidant in ryegrass. – Plant Soil **225**: 193-200, 2000.

Hasanuzzaman M., Fujita M.: Selenium pretreatment upregulates the antioxidant defense and methylglyoxal detoxification system and confers enhanced tolerance to drought stress in rapeseed seedlings. – Biol. Trace Elem. Res. **143**: 1758-1776, 2011.

Hermans C., Smeyers M., Rodriguez R.M. *et al*.: Quality assessment of urban trees: A comparative study of physiological characterisation, airborne imaging and on site fluorescence monitoring by the OJIP-test. – J. Plant Physiol. **160**: 81-90, 2003.

Jiang H.X., Yang L.T., Qi Y.P. *et al*.: Root *iTRAQ* protein profile analysis of two citrus species differing in aluminum-tolerance in response to long-term aluminum-toxicity. – BMC Genomics **16**: 949-966, 2015.

Kalaji H.M., Jajoo A., Oukarroum A. *et al*.: Chlorophyll *a* fluorescence as a tool to monitor physiological status of plants under abiotic stress conditions. – Acta Physiol. Plant. **38**: 102, 2016.

Kalaji H.M., Oukarroum A., Alexandrov V. *et al*.: Identification of nutrient deficiency in maize and tomato plants by *in vivo* chlorophyll *a* fluorescence measurements. – Plant Physiol. Bioch. **81**: 16-25, 2014.

Krüger G.H.J., De Villiers M.F., Strauss A.J. *et al*.: Inhibition of photosystem II activities in soybean (*Glycine max*) genotypes differing in chilling sensitivity. – S. Afr. J. Bot. **95**: 85-96, 2014.

Kryukov G.V., Castellano S., Novoselov S.V. *et al*.: Characterization of mammalian selenoproteomes. – Science **300**: 1439-1443, 2003.

Łabanowska M., Filek M., Kościelniak J. *et al*.: The effects of short-term selenium stress on Polish and Finnish wheat seedlings – EPR, enzymatic and fluorescence studies. – J. Plant Physiol. **169**: 275-284, 2012.

Lambers H. Chapin III F.S., Pons T.L.: Plant Physiological Ecology. 2nd Edition. Pp. 604. Springer-Verlag, New York 2008.

Lavergne J., Leci E.: Properties of inactive photosystem II centers. – Photosynth. Res. **35**: 323-343, 1993.

Lichtenthaler H.K.: Chlorophylls and carotenoids: Pigments of photosynthetic biomembranes. – Method. Enzymol. **148**: 350-382, 1987.

Lin Z.H., Chen L.S., Chen R.B. *et al*.: CO_2 assimilation, ribulose-1,5-biphosphate carboxylase/oxygenase, carbohydrates and photosynthetic electron transport probed by the JIP-test, of tea leaves in response to phosphorus supply. – BMC Plant Biol. **9**: 43, 2009.

Lindblom S.D., Valdez-Barillas J.R., Fakra S.C. *et al*.: Influence of microbial associations on selenium localization and speciation in roots of *Astragalus* and *Stanleya* hyperaccumulators. – Environ. Exp. Bot. **88**: 33-42, 2013.

Martins J.P.R., Martins A.D., Ferreira Pires M.F. *et al*.: Anatomical and physiological responses of *Billbergia zebrina* (Bromeliaceae) to copper excess in a controlled microenvironment. – Plant Cell Tiss. Org. **126**: 43-57, 2016.

Martins R.F.A., Souza A.F.C., Pitol C., Falqueto A.R.: Physiological responses to intense water deficit in two genotypes of crambe (*Crambe abyssinica* Hochst.). – Aust. J. Crop Sci. **11**: 821-827, 2017.

Mehta P., Jajoo A., Mathur S., Bharti S.: Chlorophyll *a* fluorescence study revealing effects of high salt stress on Photosystem II in wheat leaves. – Plant Physiol. Bioch. **48**: 16-20, 2010.

Murashige T., Skoog F.: A revised medium for rapid growth and bio-assays with tobacco tissue cultures. – Physiol. Plantarum **15**: 473-497, 1962.

Ning N., Yuan X.Y., Dong S.Q. *et al*.: Increasing selenium and yellow pigment concentrations in foxtail millet (*Setaria italica* L.) grain with foliar application of selenite. – Biol. Trace Elem. Res. **170**: 245-252, 2016.

Oukarroum A., Bussotti F., Goltsev V. *et al*.: Correlation between reactive oxygen species production and photochemistry of photosystems I and II in *Lemna gibba* L. plants under salt stress. – Environ. Exp. Bot. **109**: 80-88, 2015.

Oukarroum A., Madidi S.E.L., Schansker G., Strasser R.J.: Probing the responses of barley cultivars (*Hordeum vulgare* L.) by chlorophyll *a* fluorescence OLKJIP under drought stress and re-watering. – Environ. Exp. Bot. **60**: 438-446, 2007.

Oukarroum A., Schansker G., Strasser R.J.: Drought stress effects on photosystem I content and photosystem II thermotolerance analyzed using Chl *a* fluorescence kinetics in barley varieties differing in their drought tolerance. – Physiol. Plantarum **137**: 188-199, 2009.

Owusu-Sekyere A., Kontturi J., Hajiboland R. *et al*.: Influence of selenium (Se) on carbohydrate metabolism, nodulation and growth in alfalfa (*Medicago sativa* L.). – Plant Soil **373**: 541-552, 2013.

Paillotin G.: Movement of excitations in the photosynthetic domains of photosystem I. – J. Theor. Biol. **58**: 337-352, 1976.

Pilon-Smith E.A.H., Quin C., Tapken W. *et al*.: Physiological functions of beneficial elements. – Curr. Opin. Plant Biol. **12**: 267-274, 2009.

Pilon-Smits E.A.H., LeDuc D.L.: Phytoremediation of selenium using transgenic plants. – Curr. Opin. Biotech. **20**: 207-212, 2009.

Pollastrini M., Nogales A.G., Benavides R. *et al*.: Tree diversity affects chlorophyll *a* fluorescence and other leaf traits of tree species in a boreal forest. – Tree Physiol. **37**: 199-208, 2017.

Qing X., Zhao X., Hu C. *et al*.: Selenium alleviates chromium toxicity by preventing oxidative stress in cabbage (*Brassica campestris* L. ssp. Pekinensis) leaves. – Ecotox. Environ. Safe. **114**: 179-189, 2015.

Redillas M.C.F.R., Strasser R.J., Jeong J.S. *et al.*: The use of JIP test to evaluate drought-tolerance of transgenic rice overexpressing *OsNAC10*. – Plant Biotechnol. Rep. **5**: 169-175, 2011.

Schansker G., Srivastava A., Govindjee, Strasser R.J.: Characterization of the 820-nm transmission signal paralleling the chlorophyll *a* fluorescence rise (OJIP) in pea leaves. – Funct. Plant Biol. **30**: 785-796, 2003.

Schansker G., Tóth S.Z., Strasser R.J.: Methylviologen and dibromothymoquinone treatments of pea leaves reveal the role of photosystem I in the Chl *a* fluorescence rise OJIP. – BBA-Bioenergetics **1706**: 250-261, 2005.

Seppänen M., Turakainen M., Hartikainen H.: Selenium effects on oxidative stress in potato. – Plant Sci. **165**: 311-319, 2003.

Stadtman T.C.: Selenocysteine. – Annu. Rev. Biochem. **65**: 83-100, 1996.

Strasser B.J., Strasser R.J.: Measuring fast fluorescence transient to address environmental questions: The JIP-test. – In: Mathis P. (ed.): Photosynthesis: From Light to Biosphere. Pp. 977-980. Kluwer Academic Publishers, Dordrecht 1995.

Strasser B.J.: Donor side capacity of Photosystem II probed by chlorophyll *a* fluorescence transients. – Photosynth. Res. **52**: 147-155, 1997.

Strasser R.J., Srivastava A., Tsimilli-Michael M.: The fluorescence transient as a tool to characterize and screen photosynthetic samples. – In: Yunus M., Pathre U., Mohanty P. (ed.): Probing Photosynthesis: Mechanisms, Regulation and Adaptation. Pp. 445-483. Taylor and Francis, London 2000.

Strasser R.J., Tsimilli-Michael M., Qiang S., Goltsev V.: Simultaneous *in vivo* recording of prompt and delayed fluorescence and 820-nm reflection changes during drying and after rehydration of the resurrection plant *Haberlea rhodopensis*. – BBA-Bioenergetics **1797**: 1313-1326, 2010.

Strasser R.J., Tsimilli-Michael M., Srivastava A.: Analysis of the chlorophyll *a* fluorescence transient. – In: Papageorgiou G.C., Govindjee (ed.): Chlorophyll *a* Fluorescence: A Signature of Photosynthesis. Advances in Photosynthesis and Respiration. Pp. 321-362. Springer, Dordrecht 2004.

Strauss A.J., Krüger G.H.J., Strasser R.J., Heerden P.D.R.V.: Ranking of dark chilling tolerance in soybean genotypes probed by the chlorophyll *a* fluorescence transient O-J-I-P. – Environ. Exp. Bot. **56**: 147-157, 2006.

Tang H., Liu Y., Gong X. *et al*.: Effects of selenium and silicon on enhancing antioxidative capacity in ramie (*Boehmeria nivea* L. Gaud.) under cadmium stress. – Environ. Sci. Pollut. R. **22**: 9999-10008, 2015.

Tausz M., Hietz P., Briones O.: The significance of carotenoids and tocopherols in photoprotection of seven epiphytic fern species of a Mexican cloud forest. – Aust. J. Plant Physiol. **28**: 775-783, 2001.

Terry N., Zayed A.M., De Souza M.P., Tarun A.S.: Selenium in higher plants. – Annu. Rev. Plant Phys. **51**: 401-432, 2000.

Tian M., Xu X., Liu Y. *et al*.: Effect of Se treatment on glucosinolate metabolism and health-promoting compounds in the broccoli sprouts of three cultivars. – Food Chem. **190**: 374-380, 2016.

Tóth S.Z., Nagy V., Puthur J.T. *et al*.: The physiological role of ascorbate as photosystem II electron donor: Protection against photoinactivation in heat-stressed leaves. – Plant Physiol. **156**: 382-392, 2011.

Tsimilli-Michael M., Strasser R.J.: *In vivo* assessment of stress impact on plants' vitality: applications in detecting and evaluating the beneficial role of mycorrhization on host plants. – In: Varma A. (ed.): Mycorrhiza. State of the Art, Genetics and Molecular Biology, Eco-Function, Biotechnology, Eco-Physiology, Structure and Systematics. 3rd edition. Pp. 679-703. Springer, Berlin-Heidelberg 2008.

Tsimilli-Michael M., Strasser R.J.: The energy flux theory 35 years later: formulations and applications. – Photosynth. Res. **117**: 289-320, 2013.

Turakainen M., Hartikainen H., Ekholm P., Seppänen M.M.: Distribution of selenium in different biochemical fractions and raw darkening degree of potato (*Solanum tuberosum*) tubers supplemented with selenate. – J. Agr. Food Chem. **54**: 8617-8622, 2006.

Vítová M., Bišová K., Hlavová M. *et al.*: Glutathione peroxidase activity in the selenium-treated *alga Scenedesmus quadricauda*. – Aquat. Toxicol. **102**: 87-94, 2011.

Wang Y.D., Wang X., Wong Y.S.: Proteomics analysis reveals multiple regulatory mechanisms in response to selenium in rice. – J. Proteomics **75**: 1849-1866, 2012.

Xue T., Hartikainen H., Piironen V.: Antioxidative and growth promoting effect of selenium in senescing lettuce. – Plant Soil **237**: 55-61, 2001.

Yao X.Q., Chu J.Z., Ba C.J.: Responses of wheat roots to exogenous selenium supply under enhanced ultraviolet-B. – Biol. Trace Elem. Res. **137**: 244-252, 2010.

Yusuf M.A., Kumar D., Rajwanshi R. *et al*.: Overexpression of γ-tocopherol methyl transferase gene in transgenic *Brassica juncea* plants alleviates abiotic stress: Physiological and chlorophyll *a* fluorescence measurements. – BBA-Bioenergetics **1797**: 1428-1438, 2010.

Zhang L., Ackley A.R., Pilon-Smits E.A.H.: Variation in selenium tolerance and accumulation among *Arabidopsis thaliana* accessions. – Plant Physiol. **164**: 327-336, 2007.

Zhong N., Zhong L., Hao L. *et al*.: Speciation of selenium in enriched garlic sprouts by high-performance liquid chromatography coupled with inductively coupled plasma-mass spectrometry. – Anal. Lett. **48**: 180-187, 2015.

Zhu Y.G., Pilon-Smits E.A.H., Zhao F.J. *et al*.: Selenium in higher plants: understanding mechanisms for biofortification and phytoremediation. – Trends Plant Sci. **14**: 436-442, 2009.

Zhuo Y., Qiu S., Amombo E. *et al.*: Nitric oxide alleviates cadmium toxicity in tall fescue photosystem II on the electron donor side. – Environ. Exp. Bot. **137**: 110-118, 2017.

Zushi K., Matsuzoe N.: Using of chlorophyll *a* fluorescence OJIP transients for sensing salt stress in the leaves and fruits of tomato. – Sci. Hortic.-Amsterdam **219**: 216-221, 2017.

Appendix. Abbreviations of the parameters, formulas and description of the data derived from the transient fluorescence of chlorophyll *a*. For review *see* Strasser *et al.* (2004) and Yusuf *et al.* (2010).

Fluorescence parameters	Description
Extracted fluorescence parameters	
$F_{20\mu s}$	Fluorescence intensity at 20 μs
$F_K = F_{0.3ms}$	Fluorescence intensity at 0.3 ms
$F_J = F_{2ms}$	Fluorescence intensity at 2 ms
$F_I = F_{30ms}$	Fluorescence intensity at 30 ms
$F_P = F_{300ms}$	Fluorescence intensity at 300 ms
Technical parameters	
$F_0 = F_{0.02ms}$	Initial fluorescence
$F_m = F_{300ms}$	Maximum fluorescence
$F_v = F_m - F_0$	Variable fluorescence
$M_0 = dV/dt_0 = 4 \times (F_{300\mu s} - F_0)/(F_m - F_0)$	Net rate of photosystem II closure
$V_J = (F_{2ms} - F_0)/(F_m - F_0)$	Relative variable fluorescence at 2 ms (point J)
$V_I = (F_{30ms} - F_0)/(F_m - F_0)$	Relative variable fluorescence at 30 ms (point I)
Quantum yields and probabilities	
$\varphi P_0 = F_v/F_m = TR_0/ABS = (F_m - F_0)/F_m = 1 - (F_0/F_m)$	Maximum quantum yield of primary photochemistry (at $t = 0$)
$\psi E_0 = ET_0/TR_0 = 1 - V_J$	Probability (at $t = 0$) that a trapped exciton moves an electron into the electron transport chain beyond Q_A^-
$\varphi E_0 = \varphi P_0 \times \psi E_0 = (TR_0/ABS) \times (ET_0/TR_0) = ET_0/ABS = (1 - F_0/F_m) \times (1 - V_J)$	Quantum yield of electron transport (at $t = 0$)
$\varphi D_0 = DI_0/ABS = 1 - \varphi P_0 = F_0/F_m]$	Quantum yield of energy dissipation (at $t = 0$)
$\delta R_0 = RE_0/ET_0 = (1 - V_I)/(1 - V_J)$	Efficiency/probability with which an electron from the intersystem electron carriers moves to reduce end electron acceptors at the PSI acceptor side (RE)
$\varphi R_0 = RE_0/ABS = \varphi P_0 \times \psi E_0 \times \delta R_0$	Quantum yield of reduction of end electron acceptors at the PSI acceptor side (RE)
$RC/ABS = (RC/TR_0) \times (TR_0/ABS) = (V_J/M_0) \times (F_v/F_m)$	Total number of active reaction centers per absorption
Specific energy fluxes	
$ABS/RC = M_0 \times (1/V_J) \times (1/\varphi P_0)$	Absorption flux per reaction center (RC) at $t = 0$
$TR_0/RC = M_0 \times (1/V_J)$	Trapping flux (leading to Q_A reduction) per RC at $t = 0$
$ET_0/RC = M_0 \times (1/V_J) \times \psi E_0$	Electron transport flux (further than Q_A^-) per RC at $t = 0$
$DI_0/RC = (ABS/RC) - (TR_0/RC)$	Dissipated energy flux per RC at $t = 0$
$RE_0/RC = M_0 \times (1/V_J) \times \psi E_0 \times \delta R_0$	Reduction of end acceptors at PSI electron acceptor side per RC at $t = 0$
Performance indices	
$PI_{(ABS)} = RC/ABS \times [\varphi P_0/(1 - \varphi P_0)] \times [\psi E_0/(1 - \psi E_0)]$	Performance index based on absorption
$PI_{(Total)} = PI_{ABS} \times [\delta R_0/(1 - \delta R_0)]$	Overall performance index, which measures the performance up until the final electron acceptors of PSI